Capacity losses due to solid electrolyte interphase formation and sodium diffusion in sodium-ion batteries

Le Anh Ma
Uppsala University https://orcid.org/0000-0002-2293-1901
Alexander Buckel
Uppsala University
Leif Nyholm
Uppsala University https://orcid.org/0000-0001-9292-016X
Reza Younesi (reza.younesi@kemi.uu.se)
Uppsala University https://orcid.org/0000-0003-2538-8104

Article

Keywords: Carbonate Electrolyte Systems, Electrochemical Testing, Synchrotron-based X-ray Photoelectron Experiments, Galvanostatic Cycling Protocols, Na-trapping Effect

Posted Date: June 30th, 2021

DOI: https://doi.org/10.21203/rs.3.rs-623903/v1

Abstract

Knowledge about capacity losses due to the formation and dissolution of the solid electrolyte interphase (SEI) layer in sodium-ion batteries (SIBs) is still limited. One major challenge in SIBs is the fact that the SEI generally contains more soluble species than the corresponding SEI layers formed in Li-ion batteries. By cycling carbon black electrodes against Na-metal electrodes, to mimic the SEI formation on negative SIB electrodes, this study studies the associated capacity losses in different carbonate electrolyte systems. Using electrochemical testing and synchrotron-based X-ray photoelectron (XPS) experiments, the capacity losses due to changes in the SEI layer and diffusion of sodium in the carbon black electrodes during open circuit pauses of 50 h, 30 h, 15 h and 5 h are investigated in nine different electrolyte systems. The different contributions to the open circuit capacity loss were determined using a new approach involving different galvanostatic cycling protocols. It is shown that the capacity loss depends on the interplay between the electrolyte chemistry and the thickness and stability of the SEI layer. The results show, that the Na-diffusion into the bulk electrode gives rise to a larger capacity loss than the SEI dissolution. Hence, Na-trapping effect is one of the major contribution in the observed capacity losses. Furthermore, the SEI formed in NaPF6-EC:DEC was found to become slightly thicker during 50 h pause, due to self-diffused deintercalation of Na from the carbon black structure coupled by further electrolyte reduction. On the other hand, the SEI in NaTFSI with the same solvent goes into dissolution during pause. The highest SEI dissolution rate and capacity loss was observed in NaPF6-EC:DEC (0.57 µAh/hpause) and the lowest in NaTFSI-EC:DME (0.15 µAh/hpause).

Introduction

With increasing consciousness about global warming and climate change, the demand on renewable energy technologies followed by sustainable energy storage options are increasing. In this respect, rechargeable batteries based on alkali metal ions such Li^+ and Na^+ have gained much attention for use in different applications.[1,2] It is, however, still important to ensure that the performances of these batteries are improved especially regarding their lifetime. The latter is particularly important in applications such as stationary energy storage where long battery life-times are required. Therefore, the ageing of electrodes and electrolytes as well as the influence of electrode-electrolyte interfacial reactions need to be more thoroughly comprehended.[3] For alkali-ion batteries, most non-aqueous electrolytes are unstable at the low electrode potentials of the negative electrode, which is why a passivating layer, known as the solid electrolyte interphase (SEI) layer generally is formed. Ideally, the SEI should be formed during the first cycles under minimum charge consumption to circumvent large irreversible capacity losses. The SEI layer should also be ionically conducting to facilitate the migration of alkali-ions, electronically insulating and impermeable to solvent molecules to avoid continuous solvent reduction. In addition, the SEI should be chemically inert and insoluble in the electrolyte to prevent further capacity losses as gradual SEI dissolution would result in a continuous SEI formation.[4–8]

Nevertheless, conventional alkali-ion batteries suffer from capacity losses leading to a shorter lifetime which is often due to a variety of ageing mechanisms. Those mechanisms differ between half and full-cells.[7,9,10] This work is focusing on half-cells using Na-metal electrodes and CB electrodes. In a Na-metal based half-cell, the CB electrode is capacity limiting. The charge storing capacity of the CB electrode should, however, not change as a result of SEI formation as the Na counter electrode would compensate for the SEI charge. The charge storing capacity of the CB electrode would, however, decreases during cycling as a result of Na-trapping in the CB electrode. A difference between the CB reduction and oxidation charge would thus still be seen in the presence of SEI formation, i.e., the CE would be lower than 100%. If the charge storing capacity of the CB decreases, this indicates the presence of Na-trapping. In the present case, the reduction capacities (and hence the degrees of trapping), are, however, most likely too low to be clearly seen. In other words, while the CE would be lower than 100% in the presence of SEI formation, the capacity of the CB electrode should remain the same when using a Na-metal counter electrode. It is therefore important to define the term capacity loss as a decrease in the charge storing capacity of the CB electrode or a CE value less than 100% due to SEI formation. If there is Na-trapping the CE value would be lower than 100% due to both Na trapping and SEI formation.[10,11] Hence in this work, the term “capacity loss” refers to the difference between sodiation and desodiation capacities. In a full cell such anodic capacity loss contributions are nevertheless still problematic and result in Na-depletion in the cathode, assuming it is capacity limiting.[10,11]

Ageing processes on carbon-based electrodes can be correlated to a variety of mechanisms, such as (i) SEI formation and growth resulting in initial capacity losses, (ii) gradual cracking of the electrode resulting in a loss of electric contact and hence increased cell impedance, (iii) SEI dissolution causing continuous SEI formation and (iv) Li-/Na-trapping or deintercalating at the electrode/SEI interface.[12–15] Moreover, it is often stated that the SEI formed in Na-based electrolyte systems is more soluble than their Li-counterpart. Hence, it is crucial to understand its fundamental properties in order to improve its stability.[7,16]

In our previous work, where Pt foil electrodes were used to study SEI ageing in half-cells with metallic sodium electrodes employing extended pauses for up to 50 hours after cycling at a high potential (2 V vs. Na^+/Na), the aging was found to result from SEI dissolution.[8] However, the other aforementioned ageing mechanism in half-cells related to Na-diffusion and SEI inefficiency can lead to the capacity loss at low potentials as is discussed in this work. To mimic the conditions in carbonaceous electrodes, we here used carbon black (CB) composite negative electrodes which requires consideration of additional parameters; the Na de/intercalation into CB, which is a result of the oxidation and reduction of CB under galvanostatic conditions, leading to additional capacity contributions and also charge consumption for SEI formation on a relatively high surface area of CB should be considered. Three different electrolyte salts and three different ethylene carbonate (EC) based solvent mixtures are used to systematically discuss the stability of SEI. Galvanostatic cycling combined with extended pause times stopped at different potentials under open circuit (OCV) conditions as well as synchrotron-based soft X-ray photoelectron spectroscopy

(SOXPES) are used to demonstrate the interplay between the capacity losses, SEI thicknesses and SEI compositions.

Results And Discussion

Galvanostatic cycling protocols and results. Figure 1 shows the cell setup and the galvanostatic cycling protocols used in this study to determine the capacity loss contributions, i.e., Na-diffusion and SEI reformation/dissolution. The tested electrolyte systems are shown in Table 1. CB electrodes were cycled against Na-metal in half cells containing non-aqueous electrolytes and Na-conductive β-alumina separators to prevent crosstalk between the Na and CB electrodes (see Fig. 1a).[17] The influence of crosstalk when using conventional separator such as Solupor® is shown in the Supplementary Fig. S1. The different behaviours seen for the separators show that there is diffusion of SEI species from the Na electrode to the CB electrode in the absence of β-alumina separators. Using Na-metal as the counter electrode means unlimited source of Na^+ which means that the obtained capacity should stem solely from the sodiation/desodiation of the CB electrode and the reduction of the electrolyte. Three cycling protocols were used in which each cell first was cycled with a constant current of 50 mA (63.7 mA/cm^2) five times between 0.1 and 2.0 V vs. Na^+/Na (all potentials are hereafter reported vs. Na^+/Na) and then paused at either 0.1 or 2.0 V and finally subjected to a 50-hour open circuit pause (see Fig. 1b). While longer open circuit pauses could have been used, the abovementioned pause was found to be are sufficiently long to observe noticeable capacity losses. The purpose of such open circuit pause testing at different potentials is to determine the capacity loss portions due to Na-diffusion or SEI reformation/dissolution. The lower cut-off potential was set to allow the assessment of electrolyte reduction and Na-insertion into the CB, whereas the upper cut-off voltage was set to mimic the general potential window used to study negative electrode materials.

The three cycling protocols used here enabled us to identify the capacity loss due to Na-diffusion and SEI reformation/dissolution (Fig. 1c). In the first protocol (Protocol 1, Fig. 1b), where the cell was first paused for 50 h at 0.1 V and then discharged again to 0.1 V after the pause (see Fig. 1b), the measured additional discharge capacity after the 50 h pause (DCh-AP) should then be due to reinsertion of Na^+ due to i) reaction of the reduced carbon with the electrolyte to reform the SEI (counteracting SEI dissolution) during the open circuit pause and ii) due to diffusion of Na, i.e., Na^+ and e^-, into the bulk of the CB electrode during the open circuit period (Na-trapping), which can result in a decrease Na^+ concentration at the surface of the CB electrode which allows additional Na^+ to be inserted at 0.1 V after the open circuit pause. Such trapping has been reported before in lithium-based batteries.[10] In the second protocol (Protocol 2, Fig. 1b), the CB electrode was paused at low potential of 0.1 V and then desodiated. The difference between the oxidation capacity before pause (Ch-BP) and after the pause (Ch-AP) can reveal the amount of the inability to oxidise the CB fully after the open circuit pause due to Na-diffusion resulting in Na-trapping and SEI reformation by reduced carbon as shown in Fig. 1c. During the open circuit pause Na (i.e., Na^+ and e^-) will diffuse from within the CB surface region further into the CB electrode. This makes some of the Na (i.e., Na^+ and e^-) inaccessible during the subsequent desodiation

step. This effect is hence analogous to the Li-trapping effect seen for e.g., Si, Al, Sn and TiO_2 electrodes.[9,18] Reformation of the SEI under the open circuit conditions can be obtained by the reduced carbon reducing the electrolyte. Therefore, protocol 1 and 2 should measure the same ageing processes. In the third protocol (Protocol 3, Fig. 1b), where the cell was paused at high potential of 2 V and then was discharged, the measured discharge capacity after the pause (HPS-DCh) is attributed to the re-insertion of Na into the CB structure and reformation SEI in case of SEI dissolution during the pause. In this case the CB electrode is oxidised prior to the open circuit pause and subsequently reduced. During the open circuit period there should hence only be SEI dissolution as the oxidised CB electrode cannot reduce the electrolyte Therefore, the difference between the discharge capacity before pause (DCh-BP) and after pause (DCh-AP) can determine the capacity loss mostly due to SEI dissolution (see Fig. 1c).

The Na-trapped in the electrode during previous cycling can most likely be neglected. Compared to the first and the second protocols, the third protocol has no influence from intercalated Na in the CB electrode during pause, because the cell is stopped at high potential.

Table 2 presents a summary of the capacity losses for two different electrolytes, i.e., 1 M $NaPF_6$ in EC:DEC and 1 M NaTFSI in EC:DEC obtained with the aforementioned cycling protocols as well as the associated uncertainties, based on pooled standard deviations (6 groups and 3 replicates each) asumming all the samples have the same variance. The results from the second and the third cycling protocols show similar values for both electrolytes taking the pooled standard deviation into consideration, however, the capacity loss obtained with the second protocol is clearly larger than that in found when using the third protocol. Overall, the cells with both electrolytes lost similar amounts of capacity due to the SEI dissolution at high potential (about 8 to 9 mAh measured from protocol 3) and due to Na-loss (about 24 mAh measured from protocol 2) during the 50-hour open circuit pause.

When stopped at higher potentials, as in the third cycling protocol, the capacity losses due to SEI dissolution in $NaPF_6$.EC:DEC and NaTFSI-EC:DEC were similar (approx. 8-9 mAh after the 50-hour open circuit pause), which could be a result of similar SEI properties at high potentials indicating the strong dependence on the solvent chemistry. The SEI dissolution rate should be independent of the potential. At a low open circuit potential there would also be SEI formation as the CB electrode can reduce the electrolyte. The latter cannot be the case at the higher open circuit potential as the CB electrode then is not a reducing agent. However, at higher potentials, the soluble species at the SEI surface could go into dissolution due to the absence of reduction potential, which could result into a different SEI surface chemistry and hence stability.

The first and second protocols should hence measure the same thing, i.e., the sum of Na-loss due to Na-trapping and SEI reformation. With regards of the pooled standard deviation, the differences are not significant, but can indicate a slight lower stability of SEI in $NaPF_6$-EC:DEC compared to that in NaTFSI-EC:DEC according to protocol 1. The difference between the first (and second) and the third protocol should only be due to Na diffusion. Procedure 3 should only measure the SEI dissolution charge. The

differences between the results for the first and third procedures are about 26 and 19 uAh, respectively. These results hence indicate that the main capacity loss stems from Na-loss in the CB electrode.

However, to determine the amount of capacity loss due to Na-loss and changes in the SEI at the low potentials further experiments were performed, following the cycling protocol 1.

Figure 2a shows that the first cycling protocol was used for different open circuit pause times of 50, 30, 15 and 5 hours. An indication of Na-trapping in the CB electrode is seen in Supplementary Fig. S2a, where an oxidation capacity is seen between 1.0-2.0 V, implying the removal of previously trapped Na in the bulk electrode (see explanation in the Supplementary Fig. S2a caption). Additionally, during the pause times, the potential increases as shown in Supplementary Fig. S2b, which can Na diffusion within the CB electrode. Figure 2b shows the capacity losses as a function of the square root of time. The linear behaviour implies diffusion controlled processes, such as Na-trapping, which has also been observed for Li systems.[9] Figure 2c suggests a linear correlation between capacity losses after 50 h pause and the electrolyte volume, *i.e.,* a larger electrolyte volume results in a larger capacity loss. Electrolyte volume cannot influence the Na-diffusion in a bulk electrode, and hence, this is only related to SEI dissolution. This indicates that SEI dissolution has a clear impact on the total capacity loss observed after the open circuit pause. The capacity loss at zero electrolyte volume should therefore indicate the capacity loss stemming from Na diffusion and is 25 mAh, which is similar to the electrochemical results in Table 2.

To study the influence of the electrolyte on the capacity losses, nine different non-aqueous electrolyte systems were investigated using protocol 1. Three different Na-salts, sodium hexafluorophosphate ($NaPF_6$), sodium bis(fluorosulfonyl)imide (NaFSI) and sodium trifluoromethanesulfonmide (NaTFSI) in three different solvent mixtures in which ethylene carbonate (EC) solvent was mixed with either diethylene carbonate (DEC), propylene carbonate (PC) or 1,2-dimethoxyethane (DME) in (1:1) volumetric ratio were hence investigated (see Table 1). The capacity difference between charge and discharge can be described as irreversible capacity.[19] As shown in Supplementary Fig. S3, the charge and discharge capacities after the first cycle ranged from 50 to 90 mAh per cycle, while the irreversible capacity reached almost the zero-line after the first cycle (see Supplementary Fig. S4).To compare the charge consumption for the 1st SEI formation and the SEI reformation during the following cycles in different electrolyte systems, the irreversible capacities for different cycles are plotted in Fig. 3. The 1st irreversible charge, which is significantly larger than the rest of the irreversible capacities, can correspond to SEI formation (Fig. 3a). The highest charge consumption was observed in 1 M $NaPF_6$-EC:DEC and the lowest by 1 M NaTFSI-EC:DME. The accumulated irreversible capacity between cycles 2 and 5, which is significantly smaller than the 1st cycle irreversible capacity, shows that the EC:DME electrolytes featured the lowest accumulated irreversible capacity irrespective of the salt used. Such irreversible charge consumption between cycles 2 and 5 can be considered as further SEI formation complementary to the SEI formation during the first cycle, or most likely it can be assigned to SEI reformation to compensate the dissolved SEI during the initial cycles when the electrolyte becomes saturated by the SEI species. In general EC:DEC and EC:PC based electrolytes, for all three salt systems resulted in higher charge consumption, while in

EC:DME resulted in the lowest SEI formation charge (85-110 mAh) irrespective of the salt used. Figure 3b shows the absolute capacity loss due to self-discharge implying SEI dissolution. The largest capacity loss was observed in EC:DEC and EC:PC based electrolytes (25 – 35 mAh after a 50- hour pause). By plotting each capacity loss against the pause time (see Supplementary Fig. S5), the capacity loss rate can be obtained (see Fig.e 3c). Similar to the capacity losses after a 50-hour pause in Fig. 3b, the highest capacity loss rate was observed in the electrolyte system $NaPF_6$-EC:DEC (0.57 mAh/h_{pause}) and the lowest in NaTFSI-EC:DME (0.15 mAh/h_{pause}).

In general the choice of solvent systems has a stronger influence on the observed capacity losses than the used electrolyte salts, signifying that solvent reduction plays an important role.

There is an interdependence between the accumulated capacity due to SEI formation to absolute the capacity loss (see Fig. 3). The correlation becomes evident in $NaPF_6$-EC:DEC for example, a higher irreversible SEI capacity corresponds to a higher capacity loss during pause which can be a result of higher SEI solubility. On the other hand, NaTFSI-EC:DME exhibits significantly lower irreversible SEI capacities which resulted also in lower capacity loss rates. With regards to the electrolyte volume effect on the SEI dissolution rate and a concentration gradient along the SEI/electrolyte interphase, a larger concentration of soluble SEI species at the electrode surface leads to a higher dissolution drivin force in the respective electrolyte systems. Hence, the thicker and more porous the SEI with more soluble SEI species, the more capacity loss should be seen. The results showed the lowest irreversible charge consumption in NaTFSI in EC:DME. A low irreversible capacity indicates a thinner, more compact and a less soluble SEI during cycling compared to the other electrolyte systems.

X-ray photoelectron studies on the SEI surface. To understand how the SEI formation and its composition and stability depend on the electrolyte, synchrotron-based X-ray photoelectron spectroscopy (XPS) with photon energies of 2500 and 7500 eV was conducted. Following the galvanostatic results, the electrolyte salt systems with the highest and lowest capacity losses during the open circuit pause, i.e., $NaPF_6$ and NaTFSI in all three solvent mixtures, were studied with XPS. Supplementary Fig. S6 and S7 show XPS C 1s spectra representing the compositional SEI of the pristine CB electrode before and after a 50-hour pause for the $NaPF_6$ and NaTFSI systems, respectively.

For all surface sensitive C 1s spectra, the relative intensity of C-C peak at 284.0 eV, which corresponds to the pristine electrode decreased, and became less visible after cycling. While this confirmed the formation of a SEI layer on the surface electrodes, the C-C peak was still detectable. This indicated that the SEI was thinner than about 20 nm (this is a rough estimation of the probing depth for a photon energy of 2500 eV). The bulk sensitive spectra show a strong C-C peak at 284.0 eV, which means that the probing depth was closer to the bulk CB electrode material. In general, the bulk sensitive C 1s spectra were similar for all electrolyte systems. The C 1s spectra of all the six samples showed the presence of C-O, C-O_2, and -CO_3 species at the binding energies of 286 eV, ~287.7 eV, and 290.0 eV as the components of SEI.[2021–23] For both electrolyte salt systems, NaF was only present in the bulk SEI and not on the surface (see Supplementary Fig. S9), which is coherent with reported SEI models.[5,6,24,25] In Li-based systems, it has

been shown that more organic and semi-carbonate components are formed at the SEI/electrolyte interphase, whereas more inorganic species such as Li_2O and LiF are found at the electrode/SEI interface.[5,6,24] Such microphase construction of inorganic and organic SEI layers in Li-based electrolyte is therefore also observed for these Na-based electrolytes.[7] Overall, the XPS spectra for the samples before extended pause (all the black color spectra in Supplementary Fig. S7 to S12) display similar features for all samples.

Comparing the $NaPF_6$ and NaTFSI electrolytes, it is seen that the SEI compositions do not change significantly after the pause which could be the result of the equal and/or very little dissolution of SEI species (see Supplementary Fig. S13). With regards of the surface-sensitive probing depth of less than 20 nm and the slight peak intensity change corresponding to the CB electrode at 284.0 eV (see Supplementary Fig. S7), the extent SEI dissolution must be very little wich is in agreement with the galvanostatic results in Table 2 with protocol 3 for $NaPF_6$-EC:DEC and NaTFSI-EC:DEC. The $NaPF_6$-EC:DME electrolyte yielded the most significant compositional changes in the SEI surface after a 50-hour pause (Supplementary Fig. S13a). Generally, the SEI formed in $NaPF_6$ electrolytes show mainly carbon-oxygen species on the surface corresponding to organic and carbonate components, whereas in NaTFSI the N and S content were larger stemming from the electrolyte salt. Compared to $NaPF_6$-EC:DEC and –EC:PC, the alkoxides, carboxyl and carbonate components in the SEI of $NaPF_6$-EC:DME decrease after the pause, while the intensities for NaF and Na_2O increase. The carboxyl and carbonate components in the SEI of NaTFSI-EC:DME also undergo dissolution during the pause, yet to a smaller extent compared to its $NaPF_6$ counterpart. In comparison to the surface, the bulk SEI in NaTFSI electrolytes shows less electrolyte salt decomposition products, whereas for $NaPF_6$ systems, the bulk SEI contains more salt decomposition species resulting in higher F content (Supplementary Fig. S13).

$NaPF_6$ and NaTFSI in the worst solvent mixture, which was EC:DEC (see Fig. 3), and the best solvent mixture, EC:DME, show different trends before and after the pause. The corresponding peak of the CB electrode at 284.0 eV is decreasing for $NaPF_6$-EC:DEC and -EC:DME (see Fig. 4a and b), whereas for NaTFSI-EC:DEC and –EC:DME it is increasing (see Fig. 4c and d). That means the SEI in $NaPF_6$-EC:DEC and -EC:DME was growing during pause, which could be a result of electrolyte reduction by reduced carbon and/or gradual saturation of the electrolyte during cycling preventing more dissolution. On the other the hand in NaTFSI-EC:DEC and -EC:DME, the SEI was dissolving (approx. less than 2 nm) while paused for 50 hours. Such SEI growth during pausing has been reported before in Li-cells using carbonaceous electrodes and $LiPF_6$ based electrolytes.[26–28] Similar to $LiPF_6$, the SEI growth during pause in $NaPF_6$-EC:DEC and –EC:DME could stem from previously sodiated carbon reducing more electrolyte, forming additional SEI species. Moreover, the increase in SEI thickness by a few nanometers in the $NaPF_6$ systems are more pronounced with EC:DEC than in EC:DME, implying that the SEI in $NaPF_6$-EC:DEC is more unstable than in EC:DME and undergoing stronger changes (see Fig. 4a and b) in agreement with the electrochemical results in Fig. 3. Similarly, the peak increase in the NaTFSI systems, corresponding to

SEI dissolution, is more enhanced in EC:DEC than in EC:DME (see Fig. 4c and d), which is also conform with the electrochemical results in Fig. 3.

Hence, the XPS results confirm the trends in the electrochemical results, that EC:DEC is the worst and EC:DME is the best solvent mixture in terms of SEI stability, because the changes in the XPS spectra are more significant with EC:DEC than in EC:DME (see Fig. 4). Furthermore, the two salt systems showed different ageing mechanisms as seen in Fig. 1 and Table 2, which could also be shown with XPS results.

Conclusion

In this study, three electrolyte salts and three organic carbonate solvent mixtures have been electrochemically studied and evaluated based on their SEI formation and stability during cycling and pause. With different galvanostatic cycling protocols, the different contributions of Na-loss and SEI growth/dissolution could be identified. The method used here can easily be used for other electrolyte chemistries to evaluate capacity losses and therefore ageing of sodium-ion batteries. Furthermore, this SEI study on CB electrodes helped to understand the chemistry between electrolyte salt and solvent and its influences on the SEI stability during pause. The irreversible capacity due to SEI formation, the capacity loss caused by Na-diffusion and SEI growth/dissolution and its chemistry before and after dissolution depend on both salt and solvent chemistry of the electrolyte. An interdependence between capacity consumption upon SEI formation and capacity loss during pause was observed, suggesting a correlation between SEI thickness and dissolution driving force. Among the tested electrolyte systems, the SEI formed in EC:DME solvent mixtures exhibited the least SEI formation capacities, the lowest relative capacity losses and capacity loss rates during pause which are the most favorable electrochemical attributes. The ageing mechanisms depend on the electrolyte salts, therefore in this work, SEI growth during pause was found with $NaPF_6$ and dissolution with NaTFSI systems. The contrast in SEI behaviour between $NaPF_6$ and NaTFSI during pause could originate from the gradual electrolyte saturation with SEI species during cycling in $NaPF_6$-EC:DEC and therefore suppressing SEI dissolution. The electrochemical results show the inferior properties of $NaPF_6$-EC:DEC compared to NaTFSI-EC:DME in terms of irreversible charge consumption and capacity loss rate. This work gave an insight on how to evaluate the SEI dynamics and how to probe the SEI ageing mechanisms electrochemically and spectroscopically during pause.

Methods

Cell assembly. All processes have been conducted in an argon-filled glovebox (O_2 < 1ppm, H_2O < 1 ppm). All used solvents, ethylene carbonate (EC, Gotion), diethylene carbonate (DEC, BASF), propylene carbonate (PC, Gotion) and 1,2-dimethoxyethane (DME, BASF) have been filtered through a 0.2 mm Nylon membrane syringe filter (VWR®). The solvent mixtures EC:DEC, EC:PC and EC:DME are each prepared with volume ratio of 1:1. The electrolyte salts sodium trifluoromethanesulfonimide (NaTFSI, Aldrich) and sodium hexafluorophosphate ($NaPF_6$, Stella) were vacuum dried for 24 hours at 120 °C, whereas the

thermally less stable salt sodium bis(fluorosulfonyl)imide (NaFSI, Solvonic) was dried at 60 °C for 48 hours under vacuum. Each salt is added to the three electrolyte solvent mixtures to a concentration of 1 M (see Table 1). For the carbon black electrodes, a mixture of 0.9 g of carbon black (TIMCAL ENASCO 250P) and 0.1 g of sodium carboxymethyl cellulose (CMC, Merck) and 10 ml distilled water is ball-milled for 1 h at 600 rpm. Then the slurry is casted on carbon coated aluminum foil with a thickness of 200 mm and dried at 100 °C. Discs with 10 mm diameter are then punched and vacuum dried at 120 °C for 12 hours in the argon-filled glovebox. The average active material of ten measured electrodes is 2 ± 0.01 mg. Galvanostatic cycling tests have been carried with Na-half cells. For this, carbon black electrodes (10 mm diameter) as working electrodes have been assembled with b-alumina discs (Ionotec; 1 mm thickness; 20 mm diameter) as separator and Na-metal electrodes on aluminum foil (14 mm diameter) in a pouch cell. An illustration of the cell setup is shown in Fig. 1c. The electrolyte volume is 150 mL if not stated otherwise. For the comparison between b-alumina and Solupor separator, Solupor® Lydall – 3PO7A instead of b-alumina is used. In this study, the terms discharge and charge correspond to sodiation and desodiation of the carbon black electrodes.

Electrochemical testing. Galvanostatic experiments have been carried out with the Novonix high-precision cycler system at 30 °C. The cells have been cycled from 0.1 V to 2.0 V vs. Na^+/Na with a constant current of 50 mA. The cut-off potential was set to 0.1 V, which is slightly above 0 V to avoid underpotential deposition of sodium.[29,30] After 5 cycles, open circuit pauses are applied at 0.1 V, the sodiated state of carbon black to exclude volume changes during desodiation and possible changes in the SEI at higher voltages due to oxidation. The cycling program is shown in Fig. 1a.

Characterization XPS. For the x-ray photoelectron (XPS) measurements have been conducted at the synchrotron facility Deutsches-Elektronen-Synchrotron (DESY) in Hamburg, Germany. For this, the SEI formed in six different electrolyte systems, namely 1 M of $NaPF_6$ and NaTFSI in EC:DEC, EC:PC and EC:DME are probed. Two cycles were cycled five times for each electrolyte mixture, whereas one was stopped immediately after five cycles at 0.1 V (Before pause sample) and one after finishing a pause of 50 h (After pause sample). The cells are then disassembled in the glovebox and the carbon black electrodes are washed with 0.5 ml dimethylene carbonate (DMC, Sigma). The electrodes are sealed under vacuum for the transportation to the synchrotron facility. At DESY, the samples are measured at photon energies of 2500 eV and 7500 eV. Due to the major presence of sp^2 carbon bonds in carbon black, all spectra have been normalized to 284.0 eV and by the cross section of the particular core level and the inelastic mean free path (IMFP). With this, the elemental composition can be analyzed based on the relative intensities of the XPS spectra.[31,32]

Data availability

The datasets generated and/or analyzed during the current study are available from the corresponding author on reasonable request.

Declarations

Acknowledgements

This work was carried out with the support of the synchrotron facility DESY, instrument P22 (proposal I-20200237). L.A.M. and R.Y. acknowledge funding from the Swedish Research Council for Environment, Agricultural Sciences and Spatial Planning (Formas) via the grant 2016-01257, ÅForsk foundation via the grant 20-675 and all authors acknowledge funding from STandUP for Energy.

Author contributions

L.A.M wrote the manuscript. L.A.M and A.B carried out electrochemical and synchrotron-based XPS measurements and evaluation. R.Y. and L.N. were involved in experimental planning and project discussions. All authors helped with data interpretation. Authors declare no competing interests.

References

1. Environ, E. *et al.* In search of an optimized electrolyte for Na-ion batteries. *Energy Environ. Sci.* **5**, 8572–8583 (2012).

2. Nayak, P. K., Yang, L., Brehm, W. & Adelhelm, P. From Lithium-Ion to Sodium-Ion Batteries: Advantages, Challenges, and Surprises. *Angew. Chemie - Int. Ed.* **57**, 102–120 (2018).

3. Yabuuchi, N., Kubota, K., Dahbi, M. & Komaba, S. Research development on sodium-ion batteries. *Chem. Rev.* **114**, 11636–11682 (2014).

4. Peled, E., Golodnitsky, D. & Ardel, G. Advanced Model for Solid Electrolyte Interphase Electrodes in Liquid and Polymer Electrolytes. *J. Electrochem. Soc.* **144**, L208 (1997).

5. Peled, E. *et al.* Composition, depth profiles and lateral distribution of materials in the SEI built on HOPG-TOF SIMS and XPS studies. *J. Power Sources* **97–98**, 52–57 (2001).

6. Peled, E. & Menkin, S. Review—SEI: Past, Present and Future. *J. Electrochem. Soc.* **164**, A1703–A1719 (2017).

7. Mogensen, R., Brandell, D. & Younesi, R. Solubility of the Solid Electrolyte Interphase (SEI) in Sodium Ion Batteries. *ACS Energy Lett.* **1**, 1173–1178 (2016).

8. Ma, L. A., Naylor, A. J., Nyholm, L. & Younesi, R. Strategies for Mitigating Dissolution of Solid Electrolyte Interphases in Sodium-Ion Batteries. *Angew. Chemie Int. Ed.* **60**, 2–11 (2021).

9. Lindgren, F. *et al.* On the Capacity Losses Seen for Optimized Nano-Si Composite Electrodes in Li-Metal Half-Cells. *Adv. Energy Mater.* **9**, (2019).

10. Rehnlund, D. *et al.* Lithium trapping in alloy forming electrodes and current collectors for lithium based batteries. *Energy Environ. Sci.* **10**, 1350–1357 (2017).

11. Lindgren, F. *et al.* On the Capacity Losses Seen for Optimized Nano-Si Composite Electrodes in Li-Metal Half-Cells. *Adv. Energy Mater.* **9**, 1901608 (2019).

12. Waag, W., Käbitz, S. & Sauer, D. U. Experimental investigation of the lithium-ion battery impedance characteristic at various conditions and aging states and its influence on the application. *Appl. Energy* **102**, 885–897 (2013).

13. Vetter, J. *et al.* Ageing mechanisms in lithium-ion batteries. *J. Power Sources* **147**, 269–281 (2005).

14. Tarascon, J. M. & Armand, M. Issues and challenges facing rechargeable lithium batteries. *Nature* **414**, 359–367 (2001).

15. Lin, C., Tang, A., Mu, H., Wang, W. & Wang, C. Aging mechanisms of electrode materials in lithium-ion batteries for electric vehicles. *J. Chem.* **2015**, (2015).

16. Moshkovich, M., Gofer, Y. & Aurbach, D. Investigation of the Electrochemical Windows of Aprotic Alkali Metal (Li, Na, K) Salt Solutions. *J. Electrochem. Soc.* **148**, E155 (2001).

17. Schafzahl, L., Hanzu, I., Wilkening, M. & Freunberger, S. A. An Electrolyte for Reversible Cycling of Sodium Metal and Intercalation Compounds. *ChemSusChem* **10**, 401–408 (2017).

18. Wei, W., Ihrfors, C., Björefors, F. & Nyholm, L. Capacity Limiting Effects for Freestanding, Monolithic TiO2Nanotube Electrodes with High Mass Loadings. *ACS Appl. Energy Mater.* **3**, 4638–4649 (2020).

19. Attia, P. M., Das, S., Harris, S. J., Bazant, M. Z. & Chueh, W. C. Electrochemical Kinetics of SEI Growth on Carbon Black: Part I. Experiments. *J. Electrochem. Soc.* **166**, E97–E106 (2019).

20. Eshetu, G. G. *et al.* Electrolytes and Interphases in Sodium-Based Rechargeable Batteries: Recent Advances and Perspectives. *Adv. Energy Mater.* **10**, (2020).

21. Fondard, J. *et al.* SEI Composition on Hard Carbon in Na-Ion Batteries After Long Cycling: Influence of Salts (NaPF 6 , NaTFSI) and Additives (FEC, DMCF) . *J. Electrochem. Soc.* **167**, 070526 (2020).

22. Komaba, S. *et al.* Electrochemical Na insertion and solid electrolyte interphase for hard-carbon electrodes and application to Na-ion batteries. *Adv. Funct. Mater.* **21**, 3859–3867 (2011).

23. Eshetu, G. G. *et al.* Impact of the electrolyte salt anion on the solid electrolyte interphase formation in sodium ion batteries. *Nano Energy* **55**, 327–340 (2019).

24. Edström, K., Herstedt, M. & Abraham, D. P. A new look at the solid electrolyte interphase on graphite anodes in Li-ion batteries. *J. Power Sources* **153**, 380–384 (2006).

25. Peled, E. The Electrochemical Behavior of Alkali and Alkaline Earth Metals in Nonaqueous Battery Systems—The Solid Electrolyte Interphase Model. *J. Electrochem. Soc.* **126**, 2047–2051 (1979).

26. Yazami, R. & Reynier, Y. F. Mechanism of self-discharge in graphite-lithium anode. *Electrochim. Acta* **47**, 1217–1223 (2002).

27. Smith, A. J., Burns, J. C., Zhao, X., Xiong, D. & Dahn, J. R. A High Precision Coulometry Study of the SEI Growth in Li/Graphite Cells. *J. Electrochem. Soc.* **158**, A447 (2011).

28. Utsunomiya, T., Hatozaki, O., Yoshimoto, N., Egashira, M. & Morita, M. Self-discharge behavior and its temperature dependence of carbon electrodes in lithium-ion batteries. *J. Power Sources* **196**, 8598–8603 (2011).

29. Tchitchekova, D. S. *et al.* On the Reliability of Half-Cell Tests for Monovalent (Li + , Na +) and Divalent (Mg 2+ , Ca 2+) Cation Based Batteries . *J. Electrochem. Soc.* **164**, A1384–A1392 (2017).

30. Tanwar, M., Bezabh, H. K., Basu, S., Su, W. N. & Hwang, B. J. Investigation of Sodium Plating and Stripping on a Bare Current Collector with Different Electrolytes and Cycling Protocols. *ACS Appl. Mater. Interfaces* **11**, 39746–39756 (2019).

31. Ferreira, G. F., Pierozzi, M., Fingolo, A. C., da Silva, W. P. & Strauss, M. Tuning Sugarcane Bagasse Biochar into a Potential Carbon Black Substitute for Polyethylene Composites. *J. Polym. Environ.* **27**, 1735–1745 (2019).

32. Malmgren, S. *et al.* Comparing anode and cathode electrode/electrolyte interface composition and morphology using soft and hard X-ray photoelectron spectroscopy. *Electrochim. Acta* **97**, 23–32 (2013).

Tables

Tables 1-2 are available in the Supplementary Files.

Figures

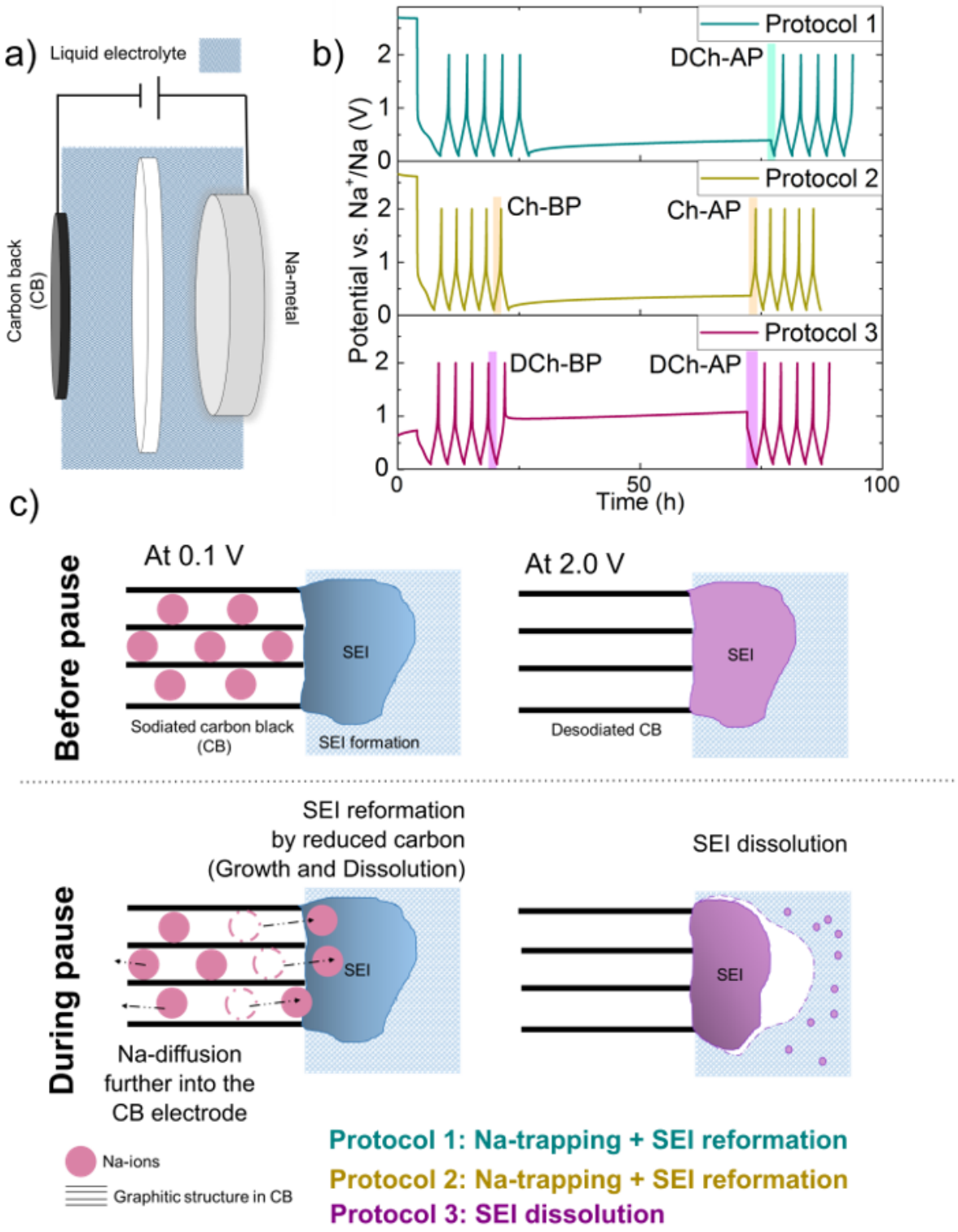

Figure 1

Galvanostatic cycling cells and protocols used to differentiate between capacity losses due to different ageing mechanisms. a) Cell setup displaying carbon black working electrode vs. Na metal counter electrode using liquid electrolyte with Na-conductive β-alumina as a separator. b) Plots of cell voltage vs. time obtained with three cycling protocols to determine capacity loss contributions. In all the protocols, the cells were cycled five times between 0.1 - 2.0 V with a current density of 63.7 μA/cm2, and then

stopped at a specific potential and relaxed for 50 hours under open circuit conditions. Protocol 1: the cells were stopped at 0.1 V, followed by open circuit relaxation and a subsequent discharging to 0.1 V. The capacity loss is determined by the discharge capacity after the pause (DCh-AP). Protocol 2: the cells were stopped at 0.1 V, followed by a 50-hour open circuit pause and a subsequent charge to 2.0 V. The capacity loss is determined by the difference between the charging capacity before (Ch-BP) and after the pause (Ch-AP). With Protocol 1 and 2, there can be diffusion of Na (i.e., Na+ and e-) inside the CB electrode resulting to Na-trapping. Protocol 3: the cells were stopped at 2.0 V, followed by a 50-hour open circuit pause and a subsequent discharge to 0.1 V. The capacity loss is calculated by the difference between the discharge capacity before (DCh-BP) and after the pause (DCh-AP). Redox reactions must then involve an reduction and oxidation of the CB electrode and a reduction of the electrolyte (i.e., SEI formation). c) Schematics ageing mechanisms during pause determined by the three different cycling options.

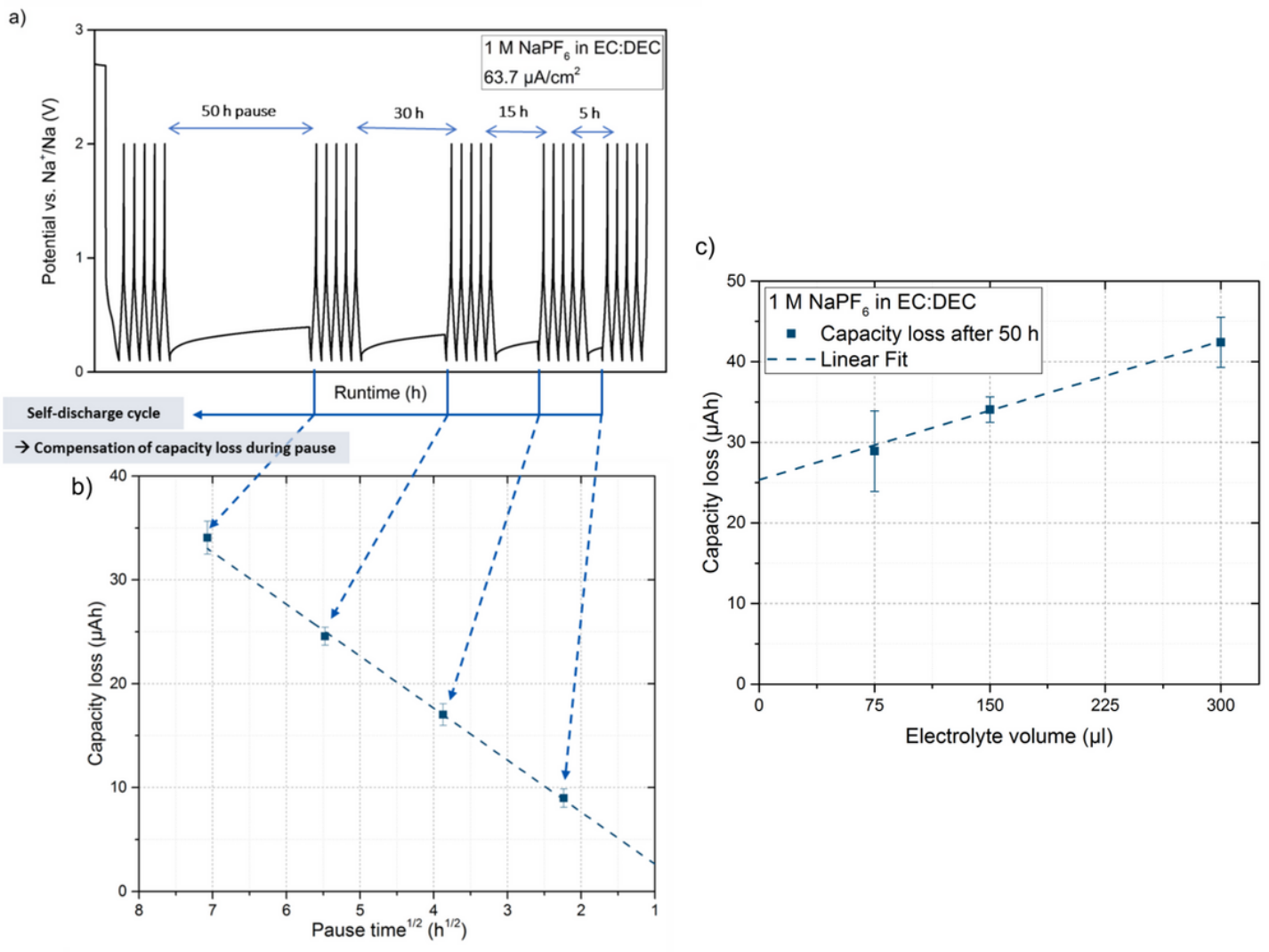

Figure 2

Galvanostatic cycling coupled with differently long open circuit pauses using 150 µl of 1 M NaPF6 dissolved in EC:DEC. a) Cycling protocol as a function of time. b) The capacity losses after each open

circuit pause as a function of the square roots of the pause times, indicating capacity losses due to diffusion controlled processes, i.e. Na-trapping. c) The capacities obtained from each self-discharge cycle after the 50 h pause as a function of different electrolyte volume. The error bars represent the standard deviations obtained based on the results for three replicate cells.

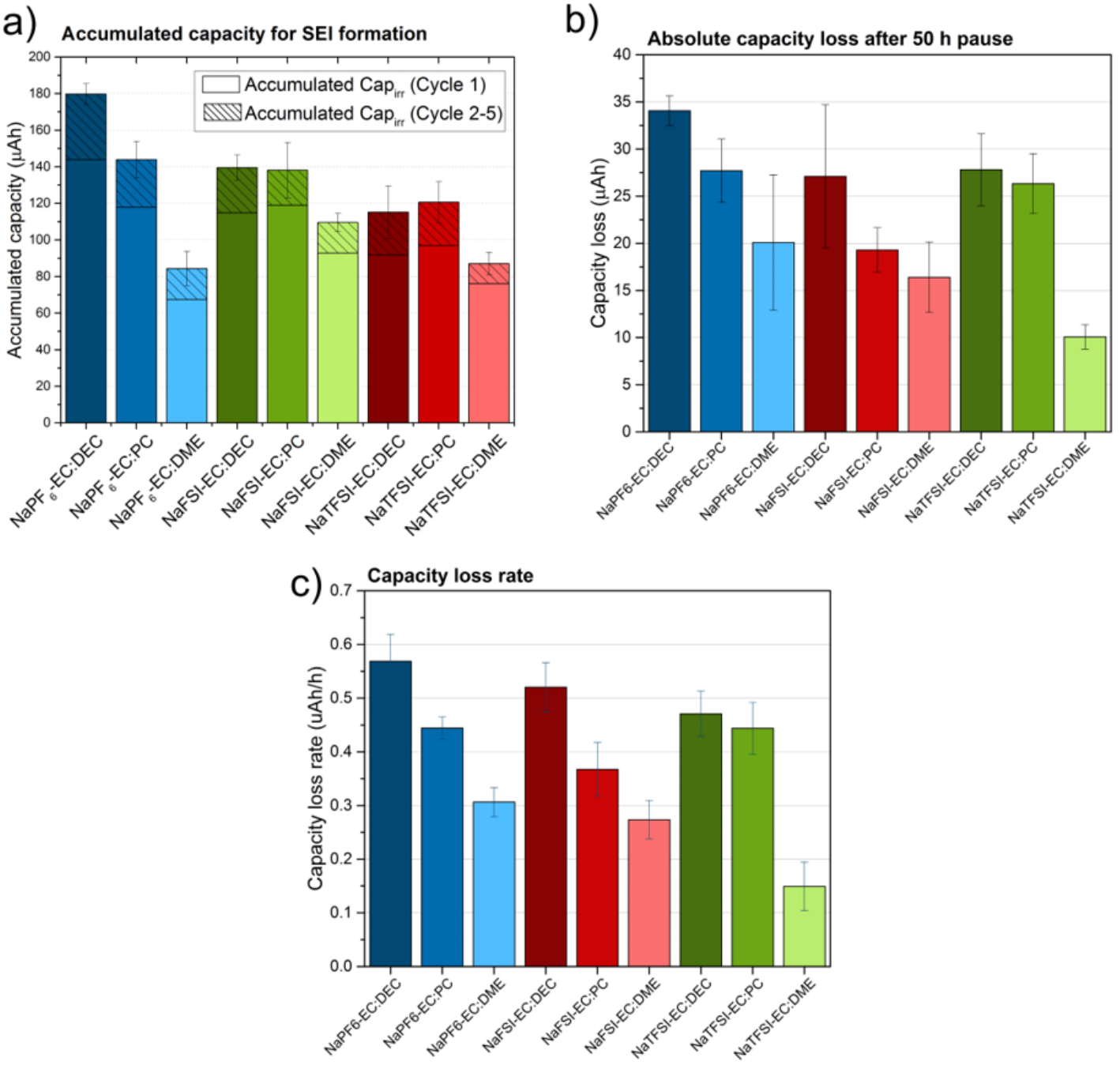

Figure 3

Galvanostatic results for the nine different electrolyte systems. The uncertainties represent the standard deviation based three replicate cells. In general, the choice of solvent shows more significant trends. a) Accumulated capacity for cycles 1 to 5 illustrating the charge needed for the SEI formation. The SEI formed in NaPF6 in EC:DEC consumed twice the capacity as consumed in NaPF6-EC:DME and NaTFSI-

EC:DME. b) Absolute capacity loss after a 50-hour pause in each electrolyte systems. The lowest absolute capacity loss is found with NaTFSI-EC:DME. c) Capacity loss rate determined from Supplementary Fig. S5. The lowest capacity loss rate was observed in NaTFSI-EC:DME with 0.15 uAh/hpause, which is almost factor four lower than the capacity loss rate in NaPF6-EC:DEC (0.57 uAh/hpause).

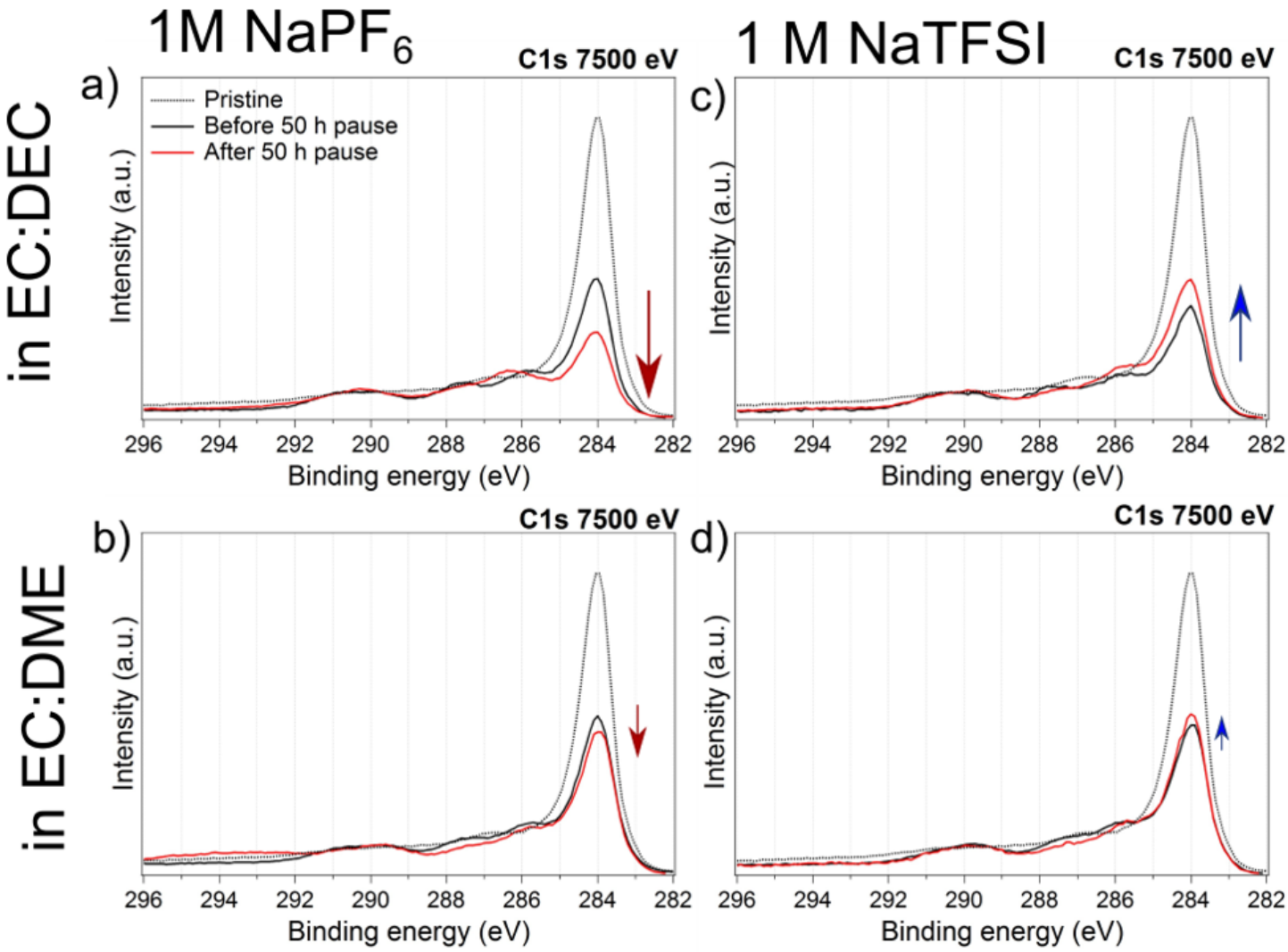

Figure 4

The decrease of the pristine CB peak at 284.0 eV in NaPF6-EC:DEC and –EC:DME indicating an SEI growth by a few nanometers after a 50-hour pause and a slight peak increase in NaTFSI-EC:DEC and –EC:DME implying a thinner SEI after pause. a) Bulk sensitive C1s spectra in NaPF6-EC:DEC and b) in NaPF6-EC:DME with peak decrease (red arrow). c) Bulk sensitive C1s spectra in NaTFSI-EC:DEC and d) NaTFSI-EC:DME with peak increase (blue arrow).

Supplementary Files

This is a list of supplementary files associated with this preprint. Click to download.

- V12SI.docx

- Table1.png
- Table2.png